JOURNAL OF MATERIALS SCIENCE 20 (1985) 1392–1406

Fracture energy of Si_3N_4

R. W. RICE*, K. R. McKINNEY, C. CM. WU, S. W. FREIMAN†, W. J. M. DONOUGH
Naval Research Laboratory, Washington, DC 20375, USA

The fracture energy of Si_3N_4 made by hot pressing, reaction sintering, and chemical vapour deposition (CVD) was studied. Extrapolation of fracture energies to zero additive or porosity levels, as well as analysis of CVD Si_3N_4 all indicate an intrinsic fracture energy of 20–30 J m^{-2}. Higher fracture energies in dense bodies with increasing additive content, or in some more porous bodies (relative to expected porosity dependence) are associated with crack branching. In dense bodies such branching may arise due to microcracking from combined effects of crack tip stresses and mismatch stresses due to differences in properties, especially thermal expansion, between Si_3N_4 and the additive or its reaction products. In porous bodies such branching appears to be due to spatial distribution of pores.

1. Introduction

There have been numerous measurements of the fracture toughness and fracture energy of Si_3N_4 and SiC due to interest in these materials for thermal-structural applications such as critical components in gas turbine engines. These measurements show that fracture energies of dense, hot pressed, Si_3N_4 (HPSN) are commonly two to three times higher than those of dense SiC. However, relatively little is understood about the basic determinants of these fracture energies and hence the source of the differences in fracture energy between these two materials, i.e. the extent to which the differences are intrinsic or extrinsic. Some evidence exists that elongated grains can increase the fracture energy of Si_3N_4 [1, 2]. There is also limited data [3, 4] supporting the general expected decrease of fracture energy of Si_3N_4 as porosity increases. However, there has been no systematic study of the fracture energy of Si_3N_4 as a function of the amount and type of hot pressing or sintering additives, and little or no measurement of the fracture energy of chemically vapour deposited (CVD) Si_3N_4. Further, there have been no studies of the interrelationship of fracture energy data of HPSN and CVD Si_3N_4, the porosity dependence of the fracture energy of reaction sintered Si_3N_4 (RSSN), or the mode of fracture of these materials.

This paper reports studies of the room temperature fracture energy of hot pressed Si_3N_4 as a function of the amount and type of additive, as well as studies of the fracture energy of CVD Si_3N_4 and RSSN. The character of cracks and fracture mode in all materials, as well as strength and Young's modulus behaviour of some materials were also determined to aid in interpreting results. While each of these studies has its uncertainties, we will show that collectively they indicate that the intrinsic fracture energy of dense, pure Si_3N_4 is in the range of 20–30 J m^{-2}, i.e. about the same as SiC [5], and that Si_3N_4 fabricated with additives are toughened by the additives, and hence may be appropriately looked upon as composites.

2. Experimental technique

Si_3N_4 was obtained from a variety of commercial and laboratory sources‡. These materials were supplemented by a substantial number of bodies

*Present address: W. R. Grace Co, Columbia, Maryland 21044, USA.
†Present address: The National Bureau of Standards.
‡RSSN of varying amount and size of pores (from burn out of various size particles from ~20 to ~200 μm average diameter) from The Boeing Co, Renton, Washington, were the predominate source of RSSN for test in this study.

0022–2461/85 $03.00 + .12

TABLE I Elastic properties of hot pressed Si_3N_4 bodies

Additives (wt %)	Density ($g\,cm^{-3}$)	Young's modulus		Poissons ratio	Source
		10^6 psi	GPa		
~ 1% MgO	3.224	46.1	318	0.273	Norton Co (NC132)
5% MgO	3.175	44.0	304	0.273	Ceradyne
5% Y_2O_3	3.258	45.2	312	0.285	Ceradyne
10% Y_2O_3	3.305	44.2	305	0.283	Ceradyne
15% Y_2O_3	3.165	43.9	302	0.270	Ceradyne
10% SiO_2	3.082*	41.2	284	0.253	This work
20% SiO_2 + 3% MgO	2.792†	29.3	202	0.247	This work
8% ZrO_2	3.201	43.4	300	0.280	This work
12% $ZrSiO_4$	3.300	42.9	296	0.278	This work

*Stereological measurements indicated ~ 0.5 to 1% porosity.
†Stereological measurements indicated ~ 4 to 5% porosity. Correction for this porosity would raise Young's modulus of a fully dense body of this composition by ~ 15%.

hot pressed§ with varying single or combined additives in our own laboratory. K_{IC} was measured using double cantilever beam (DCB) specimens with the applied moment loading technique [7]. Specimens typically had dimensions of approximately 1 cm in width, 3 to 4 cm in length, and 2 mm in thickness¶. A crack guiding groove, approximately 1 mm in width and approximately half the specimen thickness was machined down the centre of one side of the specimen¶. Cracks were initiated either from a notch, approximately 0.5 cm long and ~ 1 mm wide sawn in one end of the specimen, or from a sharp crack introduced at the base of the notch. (No differences were observed in the two techniques.) For most hot pressed bodies the plane of crack propagation was perpendicular to the hot pressing direction while for most RSSN and all CVD bodies the plane of crack propagation was parallel with cold pressing and deposition directions respectively. The nature of cracks in some DCB specimens while under load, but with the crack stationary, were observed by optical and microradiographic techniques [8, 9]. These, as well as all other, measurements were typically made at ~ 22° C and ~ 40% relative humidity.

Fracture energy (γ) values of hot pressed Si_3N_4 bodies were calculated assuming a Young's modulus (E) of 310 GPa since all such bodies used had little, or no, porosity. (However, later E values of some of these bodies were measured by a pulse echo technique as discussed later since composition was found to effect E more than first suspected.) For RSSN bodies E was determined by either a pulse echo technique or use of strain gauges on flexure specimens. Strengths were measured on many specimens in three point flexure (1.8 cm span, cross head speed $1.8\,mm\,min^{-1}$) using bars ~ 1 × 2 mm in cross-section machined from arms of the DCB specimens. Densities of RSSN specimens were determined by water immersion and the per cent porosity calculated based on a theoretical density of $3.2\,g\,cm^{-3}$. Scanning electron microscopy was used to examine fracture surfaces.

3. Experimental results

Fracture energies of a variety of HPSN bodies having essentially zero porosity are shown as a function of the volume percent additive in Figs. 1 to 3. Note that these data include measurements on all of the commonly available commercial materials and that many materials with different combinations of additives are also represented. The primary fracture mode of all of these materials was intergranular (Fig. 4). Young's modulus and other pertinent data of some bodies hot pressed with additives are given in Table I.

Figs. 5 and 6 present respectively our K_{IC} and γ results, as well as literature values [10–16] of RSSN as a function of the volume fraction porosity. Use of K_{IC} data allows evaluation of data where E values were unmeasured or unreported. Use of γ data allows incursion of other, e.g. work of fracture (WOF) data (plotted directly in Fig. 5) and also more clearly allows identification of a major source

§Hot pressed in graphite dies in a N_2 atmosphere at temperatures of 1700–1900° C for ~ 1 h at ~ 35 MPa. Typically AME 85 Si_3N_4 powder was used, see [6] and Table I.
¶The CVD materials were an exception since some specimens were thinner. Results will be shown as a function of web thickness, with greater web thicknesses in thicker samples.

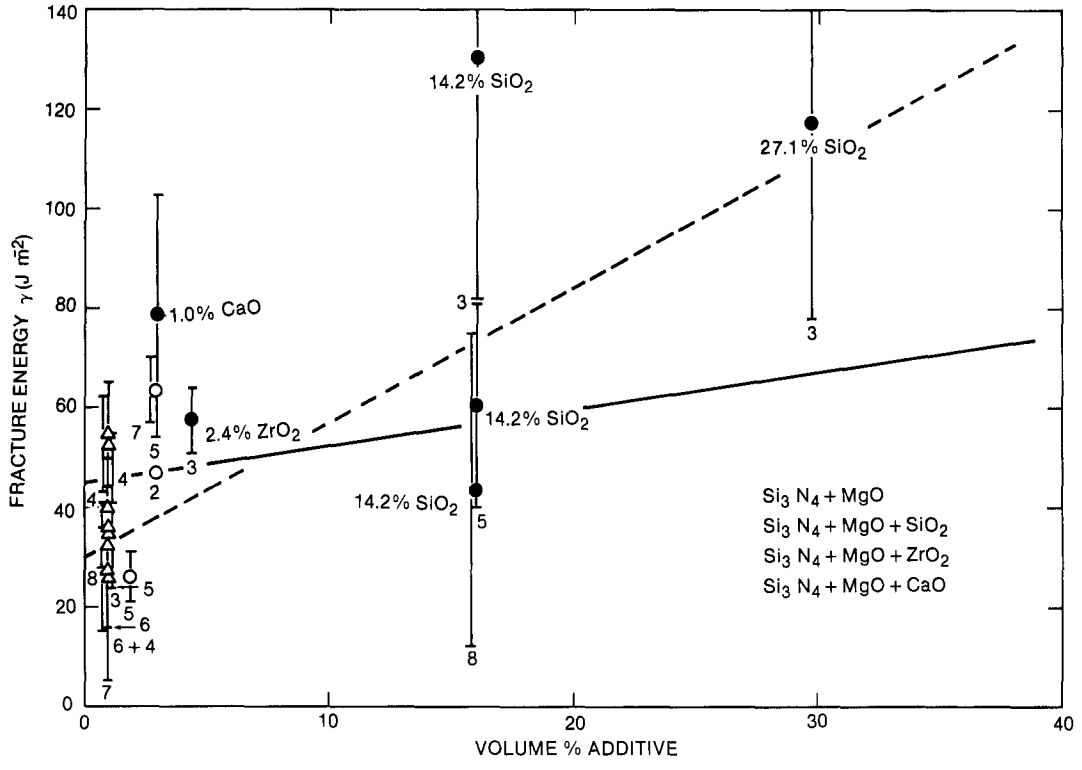

Figure 1 Fracture energy of Si_3N_4 hot pressed with MgO or MgO plus another oxide as a function of the total volume per cent additive. Vertical bars show the standard deviation and associated numbers are the number of measurements. Where more than one additive was used (solid data points), the points are plotted at the total volume % additive, and the % and type of the second additive is shown next to the data point. Note the substantial toughness that can be achieved with substantial SiO_2 additions. The solid line is a least square fit to the data at a confidence level of 95%. The dashed line is a least square fit of the data assuming a zero additive fracture energy intercept of 30 J m^{-2} is at the 99% confidence level.

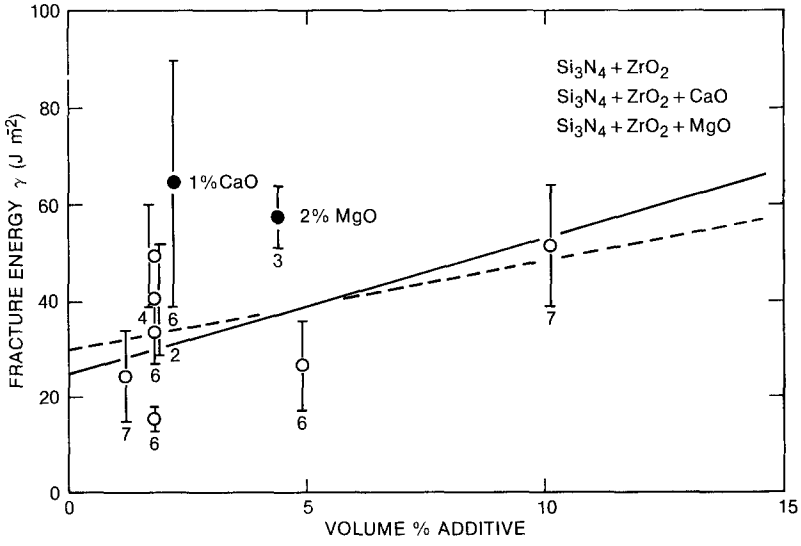

Figure 2 Fracture energy of Si_3N_4 hot pressed with ZrO_2 or ZrO_2 plus another oxide as a function of the total volume per cent of additive. Vertical bars show the standard deviation and subscripts the number of measurements. Where more than one additive is used (solid data points), the points are plotted at the total volume % additive, and the % and type of the second additive is shown next to the data point. The solid and dashed lines are least squares fits to the data assuming respectively no defined zero additive intercept and a zero additive intercept of 30 J m^{-2}. Both fits are at the 99% confidence level.

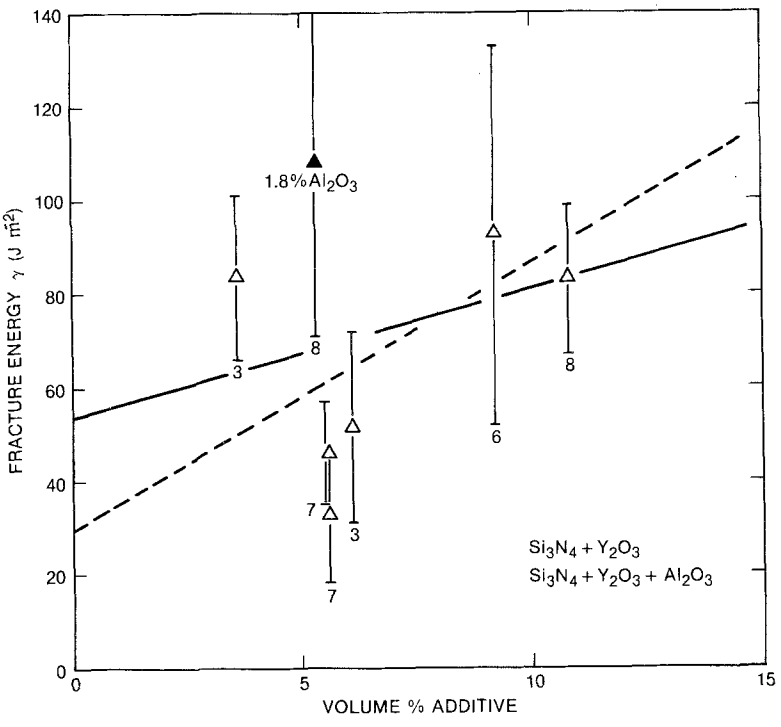

Figure 3 Fracture energy of Si_3N_4 hot pressed with Y_2O_3 or Y_2O_3 plus another oxide as a function of the total volume per cent of additive. Vertical bars show the standard deviation and subscripts the number of measurements. Where more than one additive is used (solid data points), the points are plotted at the total volume % additive, and the % and type of the second additive is shown next to the data point. The solid and dashed lines are least squares fit to the data assuming respectively no definite zero additive intercept and a zero additive intercept of 30 J m^{-2}. These fit are respectively at the 80% and 99% confidence level.

of K_{IC} and γ scatter, i.e. based on X-ray microradiography of cracks in selected samples, the γ data could be separated into two groups. The first group (A) through which lines are drawn in Fig. 6, typically showed a single simple crack, as previously reported, [8] while samples of specimens from the second group (labelled B in Fig. 5) showed two or more cracks as shown in Fig. 7*. Neither the extent of crack branching nor K_{IC} or γ showed any correlation with the size of the pores. However, higher γ values generally correlated with more or longer branches. For comparison, results of flexure strength and Young's modulus measurements as a function of porosity are shown in Figs. 8 and 9 for the same RSSN bodies along with other RSSN data [13–18]. SEM examination showed the RSSN fracture mode to be mainly transgranular (Fig. 10).

Fracture energy results for two different sources of CVD Si_3N_4 are shown in Fig. 11 as a function of web thickness. Note that 4 thin specimens from a third source†, having a web thickness of 0.4 mm, averaged 2.8 ± 1 MPa $m^{1/2}$ in agreement with the data of Fig. 11. Examination of specimens from all three sources showed fracture to be exclusively transgranular through the typically large columnar grains oriented parallel to the web thickness (Fig. 12). The large columnar grain structure of the UTRC and DCI materials was fairly uniform across the test web of the DCB specimens. The General Electric Company (GE) material graded from a finer columnar, to a larger columnar grain size, such that much of the DCB web had finer grains than the DCI or UTRC materials. X-ray microradiography and optical examination showed primarily a single crack with limited, or no, wandering and branching. Strengths of samples of these CVD materials are shown in Table II.

TABLE II Room temperature flexural strengths of CVD Si_3N_4

Strength		Number of tests	Source
10^3 psi	MPa		
17 ± 6	110 ± 40	5	General Electric
32 ± 2	220 ± 20	6	Deposits and Composites Inc
21 ± 3	150 ± 20	18	Deposits and Composites Inc

*Such crack branching is not to be confused with the branching that occurs at high crack velocities. The present observations are on stationary, but stressed cracks. The branching occurs at quasi-static velocities.
†Materials supplied by United Technology Research Centre (UTRC), East Hartford, Connetticut.

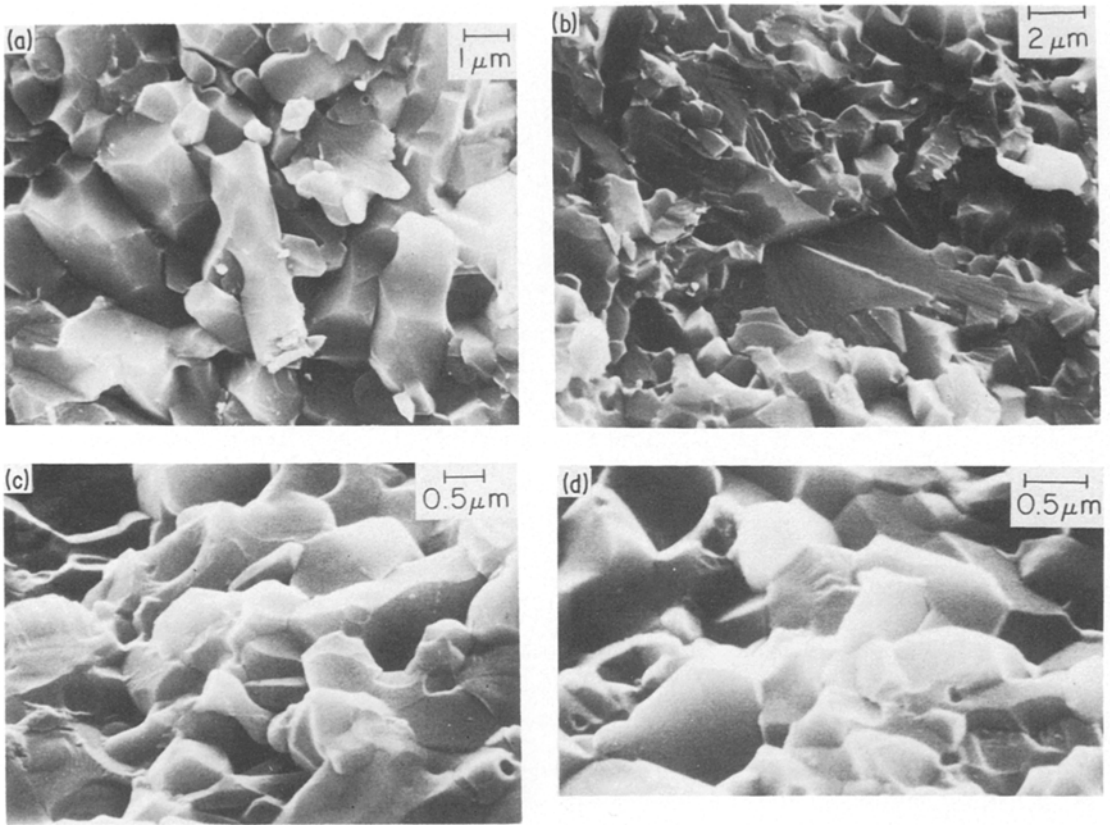

Figure 4 Fracture mode in Si_3N_4 hot pressed with ZrO_2 (a) and (b) 8 wt% ZrO_2, and (c) 2 wt% ZrO_2. Note substantial intergranular fracture, especially around elongated grains, which was also typical of Si_3N_4 bodies with other additives.

4. Discussion

4.1. Fracture energy behaviour

4.1.1. Hot pressed Si_3N_4

Consider first the fracture energy data for HPSN, which is the source of high γ values for Si_3N_4. A plot of these data as a function of the volume fraction of hot pressing additive (Figs. 1 to 3) shows substantial scatter, probably due to variations of trace porosity, distribution and degrees of reaction* of the additive phase with the Si_3N_4, impurity (especially starting oxygen) content, and grain size and shape. It was clearly impossible to conduct detailed characterization of all these parameters. Some will be discussed later. However, it is clear that fracture energy generally increases with the volume fraction of addition; e.g. least square fitting of the data in Figs. 1 to 3, show fracture energy increasing with additive level at the 80-90% confidence level. Further, the fracture energy for combined additions was typically greater than for either additive alone, again showing fracture energy to increase with the total amount of additive. Due to the scatter, extrapolations of each set of the data in Figs. 1 to 3 back to zero volume fraction addition is not particularly precise, e.g. upper and lower bounds of the data indicate fracture energy of pure dense Si_3N_4 in the range of 15 to 40 $J\,m^{-2}$. However, the HSPN data is consistent with the RSSN and CVD data which show γ to commonly be 20 to 30 $J\,m^{-2}$. Thus, for example least squares fitting of the data through a common zero additive intercept, in the more probable range, e.g. of 30 $J\,m^{-2}$ increases the confidence levels to 99% for all three sets of data. Use of 25 $J\,m^{-2}$ gives similar results.

As noted earlier, all γ values in Figs. 1 to 3 were

*The effect of variable reaction is suggested, for example, by the wide scatter of the γ values of specimens fabricated with substantial SiO_2 additions since X-ray analysis of such bodies in earlier studies of the authors showed widely varying Si_2N_2O contents in such specimens.

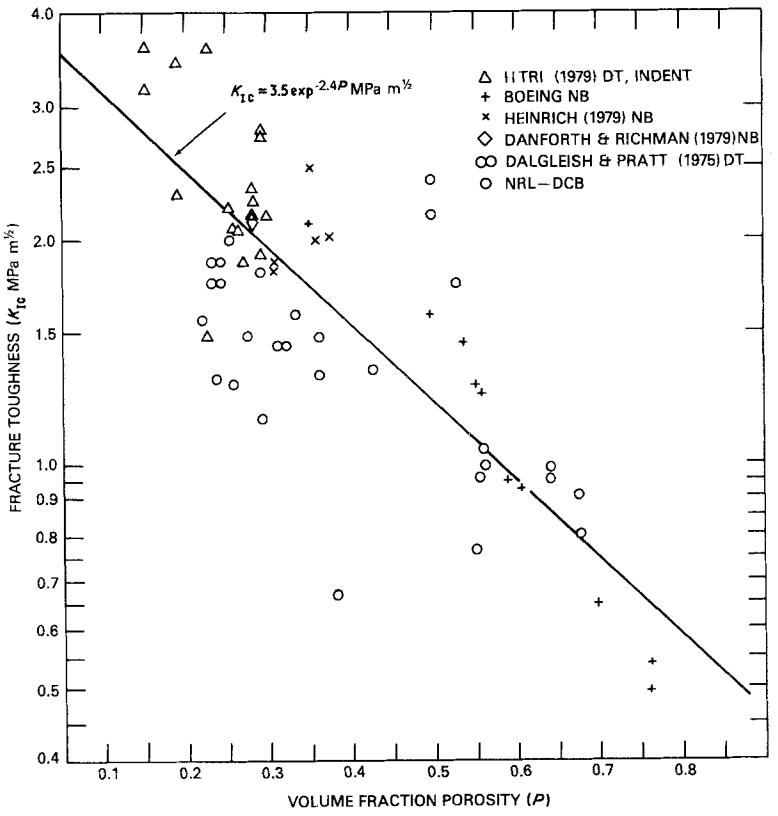

Figure 5 Fracture toughness against volume fraction porosity of RSSN. The data are from this (NRL) study (mostly on Boeing material) as well as other studies as shown. Note the least squares fitting of the exponential relationship to all the data combined. One Boeing data point of $K_{IC} = 0.21$ MPa m$^{1/2}$ at $P = 0.81$ is not shown on this graph and was not used in the above curve fitting. This excluded data point as well as three other Boeing data points for $P > 0.6$ fall progressively below the fitted line consistent with Young's modulus (Fig. 8) and strength (Fig. 9) behaviour as well as the generally expected trend from most ceramic materials [4]. The curve fitting was carried out using the actual number of measurements involved in each data point (5 on average) which are not shown here for clarity. Note also that the intercept value and the slope are probably low as discussed in the text.

calculated using $E = 310$ GPa. Subsequently it was recognized that some of the additives, especially at higher levels of additions, may have changed the E values. Results of subsequent E measurements on sample compositions are shown in Table I. These show slightly higher values of E for low additive levels, and progressively lower values for increasing levels of additives. Correction for these actual values against the constant 310 GPa used in calculating data in Figs. 1 to 3 would increase the agreement of the data with intrinsic γ of 20 to 30 J m^{-2}. Variable E from variable degrees of reactions between additives are probably another factor in the data scatter.

Other studies of HPSN containing little or no grain boundary phase corroborate the observed increases, in γ due to such phases. Palm and Greskovich [23] recently measured $\gamma = 27$ J m^{-2} for their dense HPSN made with $BeSiN_2$. Both transmission electron microscopy and high temperature strengths of these bodies show little or no grain boundary phases. Thus the single phase, dense character of these bodies and their γ value are in excellent agreement with an intrinsic γ of 20 to 30 J m^{-2}. More recently Shimada and Koizumi [24] have reported a K_{IC} of 3.8 MPa m$^{1/2}$, giving $\gamma = 24$ J m^{-2}, for dense β-Si_3N_4 hot pressed without additives under high pressure (3 GPa), in excellent agreement with the above results.

Three factors suggest that an important mechanism involved in the higher fracture toughness of Si_3N_4 bodies hot pressed with substantial additive contents is crack branching. First, X-ray microradiography clearly shows branched cracks in DCB tests of higher toughness Si_3N_4 bodies [8]. Such multiple or branched cracks most likely originate as a result of a crack interacting with mismatch stresses between grain and grain boundary phases or resultant microcracks at or near its tip. Secondly, Si_3N_4, added phases, and most of the reaction products have substantial differences in elastic moduli, and thermal expansion coefficient (factors of 3–4) or both, that lead to substantial microstructural stresses. Resultant stresses and the dimension of most of the second phase regions are sufficient to be a possible source of microcracking near the tip of stressed cracks, as observed in other composites [19]. Third, recent application of models for composites based on microcracking to these Si_3N_4 bodies results in fracture energy–composition trends similar to those observed experimentally [19]. Thus, Si_3N_4 sintered or hot pressed with additives are appropriately viewed as

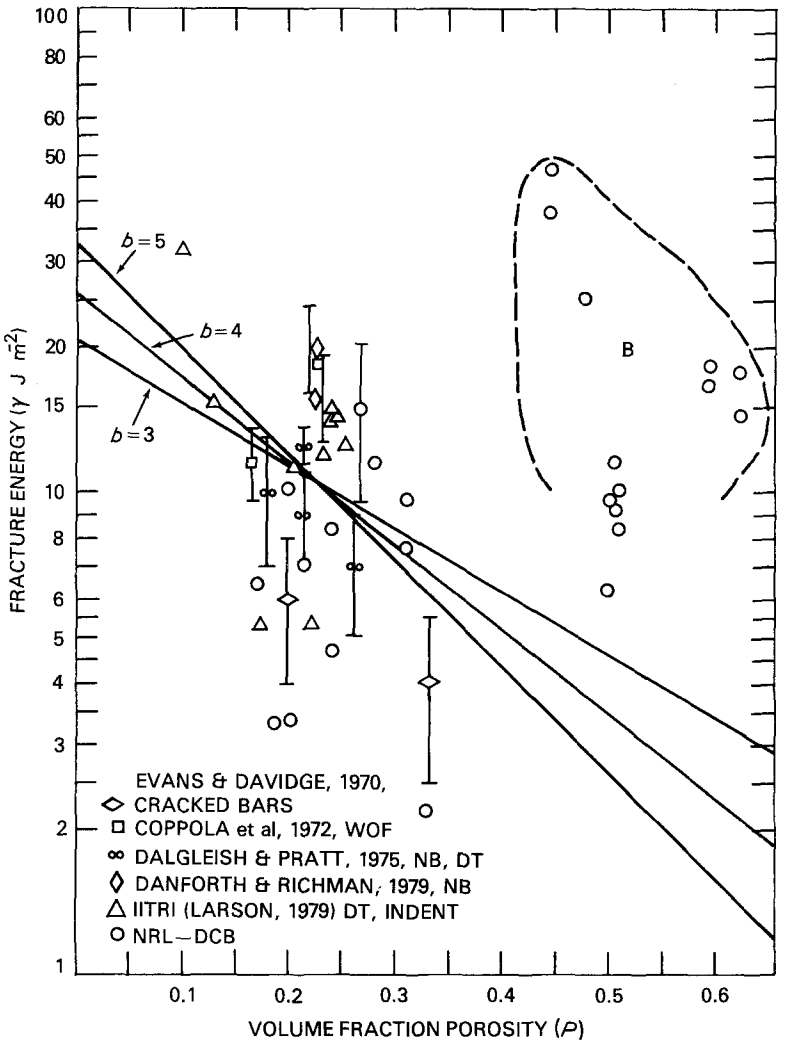

Figure 6 Fracture energy against volume fraction porosity of RSSN. The data are from this (NRL) study (mostly on Boeing material) as well as other studies as shown. The data points in the areas labelled B (all from the Boeing material) are for those types of materials for which microradiographic studies showed evidence of multiple cracks (Fig. 7). Region B (bounded by dashed lines), is not closed because of uncertainty of its lower bound. Microradiography of other specimens typically showed a single, simple crack. Note the lines drawn through the centroid of the data for $P < 0.4$ (i.e. points not in region B) with slopes (b) of 3, 4 and 5. These lines, which have slopes typical for ceramics, give fracture energy values ranging from ~ 20 to ~ 30 J m^{-2} at $P = 0$.

composites where the oxide additive not only aids densification, but also increases γ.

Grain morphology–fracture mode appears to also be a factor contributing to higher γ values in conjunction with, or instead of, microcracking. As noted earlier, increased grain elongation is associated with increased γ [1, 2]. However, grain elongation alone does not cause the increase in γ, since for example the CVD Si_3N_4 had more elongated grains, but lower fracture energies. Fracture mode is also important. Hot pressed bodies, exhibited extensive intergranular fracture, especially around elongated grains (Fig. 4) as opposed to essentially total transgranular failure for RSSN (Fig. 10) and CVD (Fig. 12) materials. Intergranular failure in the hot pressed materials is in fact central to the common concept of how elongated grains increase γ, i.e. resulting in a more tortuous crack path with mixed mode failure on the microstructural scale and associated greater total fracture area. However, the results of this study show that such intergranular fracture around elongated grains is associated with the additives. Thus, the additives also contribute to increased γ due to grain elongation.

Comparison with other materials supports the above arguments. Thus, for example, substantially elongated grains, found in some CVD SiC bodies, had little or no effect of fracture energy since cracks generally propagated transgranularly right through the elongated grains [20]. On the other hand, the fracture energy of Al_2O_3 has been reported to increase approximately in proportion to the more tortuous intergranular failure path around grains elongated along the c-axis for the cracks propagating perpendicular to the c-axis texture [21]. This is attributed to fracture energies of sapphire being $\geqslant 40$ J m^{-2}; i.e. $\geqslant 6$ times the fracture energy on most other planes [22], inhibiting transgranular

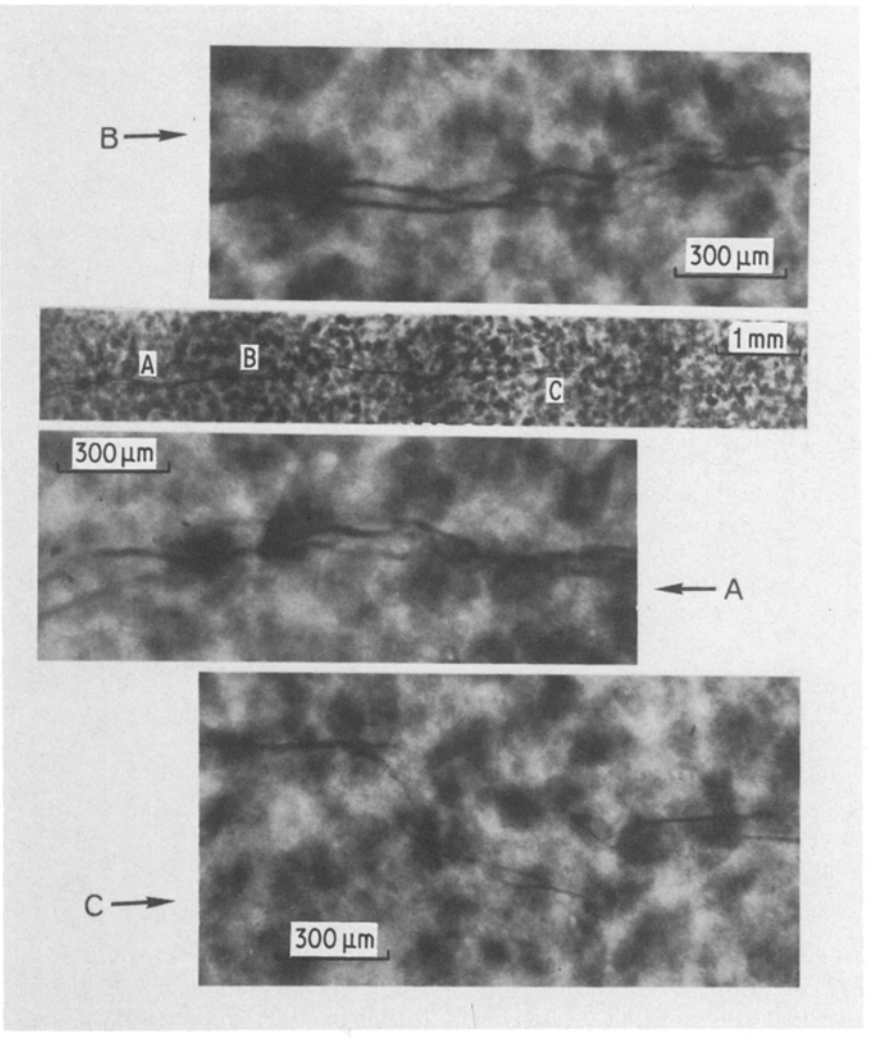

Figure 7 Microradiograph of a crack under stress in a RSSN sample showing unusually high fracture energy, $\gamma \sim 12\ J\ m^{-2}$ for its porosity ($P = 0.51$). The lower magnification shows a larger section of the stressed crack and the higher magnification photos show areas of particularly clear crack branching of deflections. The crack was branched as far to the right as it could be traced (shortly beyond the last high magnification photo). Note the general tendency for the crack to propagate from large pore to large pore (as would be expected), suggesting that the spatial distribution of these pores plays a role in such branching.

fracture approximately normal to the *c*-axis orientation of the Al_2O_3 grains, i.e. nearly on their basal planes. The resultant deflection of the cracks around the grains increases the fracture energy, but less than that required for basal plane fracture. Thus, the one probable intrinsic advantage Si_3N_4 has over SiC for higher fracture energy is the contribution that grain elongation can make to γ in Si_3N_4. Further, the analogy with Al_2O_3 and the typical elongation of Si_3N_4 grains along the *c*-axis suggests that the fracture energy on the Si_3N_4 basal plane is higher than on other planes and contributes to grain morphology–intergranular failure effects.

4.1.2. RSSN

The K_{IC} (Fig. 5) and especially γ (Fig. 6) data of RSSN also have substantial scatter which can be attributed to a variety of factors including effects of impurities (especially unreacted Si), inhomogeneous porosity distribution, and varying pore morphologies†. Variations between the data of different investigators also reflect differences in test

†Note however, this study of the Boeing material, Boeing studies of their own materials, as well as studies of Heinrich and Munz [15, 16] show little or no effect of pore size on K_{IC} or γ contrary to speculations of Danforth *et al.* [25].

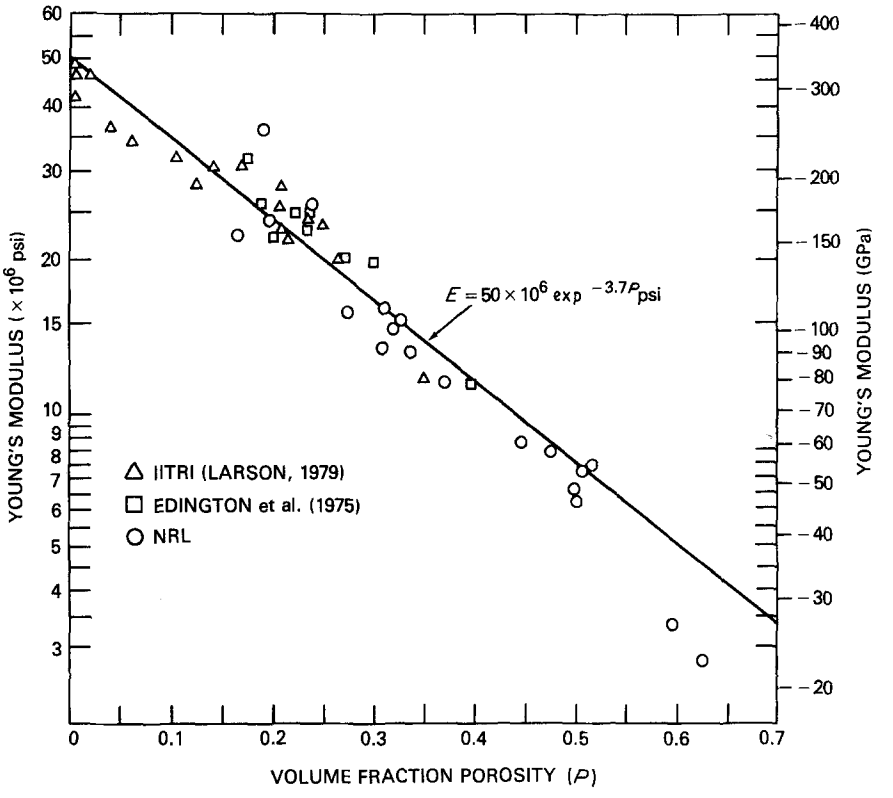

Figure 8 Young's modulus against volume fraction porosity for RSSN. Note the data from this (NRL) study includes measurements by a pulse echo as well as a strain-gauge technique (both gave very similar results). The line shown is a least square fit at the 99% confidence level. Note the points falling progressively below the line for $P > 0.6$, consistent with K_{IC} (Fig. 5) and strength (Fig. 9) data for these same materials, as well as with other ceramic data [4].

technique as discussed below. Again, while it was not possible to conduct extensive characterization to investigate all of these variables, basic trends could be identified.

The least square fitting of the RSSN K_{IC} data (Fig. 5) yields an intercept of 3.5 MPa $m^{1/2}$ which gives a γ value of ~ 20 J m^{-2}, which is reasonably consistent with, but somewhat lower than for HPSN bodies. In addition, several factors affecting the RSSN intercept can be identified, indicating probable closer agreement with the HPSN extrapolation. Larsen [14], from double torsion, controlled flaw, and indent tests, concluded that the indent results were consistently higher by ~ 5 to 100%†. Since these values are concentrated at lower porosity, they tend to give a higher intercept value. Similarly, the Boeing data were obtained by the notch beam method, using the notch as the source of sharp cracks. As the porosity decreases, there is greater uncertainty in there being adequate sharp cracks at the notch, a trend which would also tend to give too high an intercept K_{IC} value. On the other hand the high K_{IC} values at $P > 40\%$ (where P is the volume fraction porosity) in this study are typically those associated with multiple cracks (group B of Fig. 6 discussed below) which form on a scale much larger than typical strength controlling flaws. Neglecting such high values, which are not pertinent to normal strengths, would increase the slope, e.g. to 3 to 5 in better agreement with strength and E trends for RSSN (Figs. 8 and 9) and with other ceramics [4]. This increased slope would probably more than compensate for the above noted corrections lowering the K_{IC} intercept still closer to the fracture energy extrapolations for HPSN.

Specific consideration of RSSN fracture energy data allows some added (WOF) data to be included, and to more clearly illustrate the deviations at high P (group B of Fig. 6). As noted earlier, materials in group B typically showed more complex crack

†The average difference between the indent and controlled flaw tests (the two most extensively compared tests) averaged 50%. Higher values from the indent test may well result from the tendency to get the clearest readings in denser areas, e.g. because of better polishing and more definitive identification of cracks.

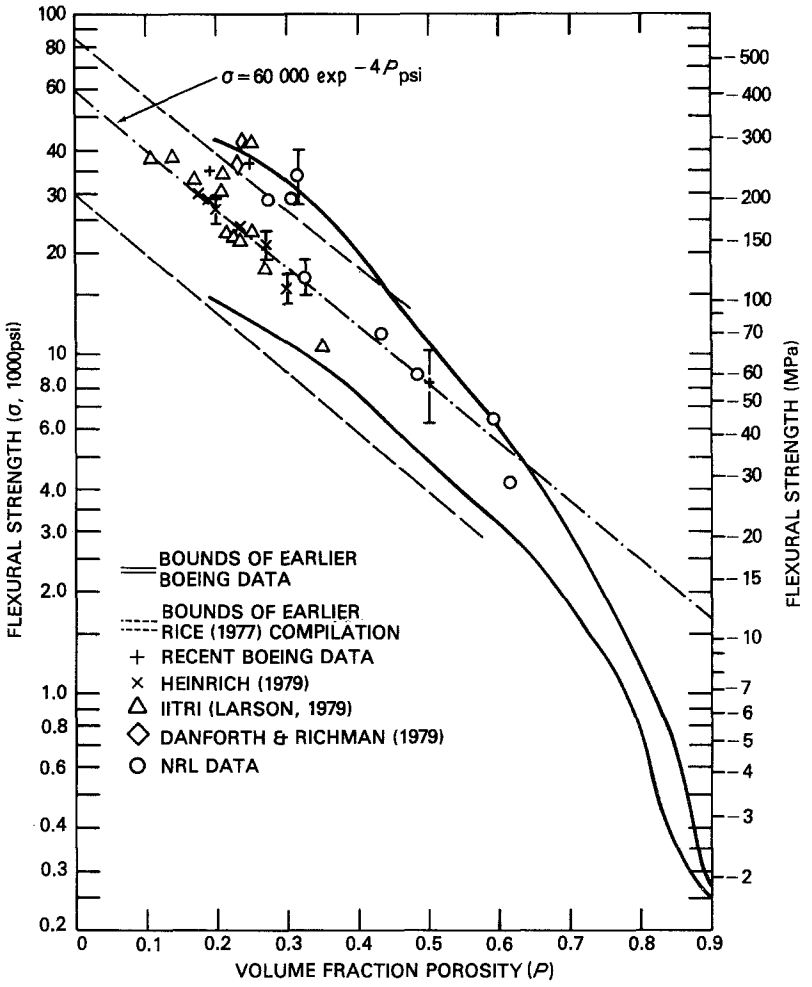

Figure 9 Flexural strength against volume fraction porosity for RSSN. Data from the present (NRL) study as well as other recent studies are shown along with the bounds for earlier data from the Boeing Co (courtesy of Mr F. Simpson). Also shown are the bounds to a previous extensive survey [17] (fitted to $\sigma = 58\,000 \exp^{-3.9P}$ psi) as well as the least square fitting of $\sigma = 60\,000 \exp^{-4.0P}$ psi to the current data (recognizing the different weightings of the data, e.g. 20 tests per points of Heinrich). The number of specimens, and most error bars are not shown for clarity, however, some sample error bars are indicated.

character, e.g. branching into two or more cracks (Fig. 7), while denser bodies typically showed only one crack. Increasing crack complexity at higher porosity is consistent with previous studies noting enhanced microcracking, crack branching, etc at higher porosity [26]. Varying degrees of this microcracking or crack branching within each group (A and B of Fig. 7) of data is probably another important source of data variation, and hence scatter, of the γ and the K_{IC} data.

Evaluation of γ data for the denser RSSN bodies, i.e. those typically characterized by a single crack (group A), supports the above analysis of K_{IC} data. While covering too narrow a porosity range and too scattered by itself to extrapolate to zero porosity, typical fracture energy–porosity behaviour can be utilized. More limited studies of RSSN [3]‡, as well as studies of other ceramic materials [4] show that the fracture energy dependence over the more typical range of porosity

‡Note that earlier studies of fracture energy and strength of RSSN as a function of porosity have commonly used hot pressed value for $P \sim 0$. These have typically given higher slopes (b values of 5 to 7) than commonly found for other ceramics. The present work shows such use of HPSN with RSSN values is not correct. The higher b values resulting from such use of HPSN data further reinforces the conclusion that strength, fracture toughness, and fracture energy (but not Young's modulus, which is more commonly decreased) are substantially increased in HPSN by the additives, i.e. as in a composite.

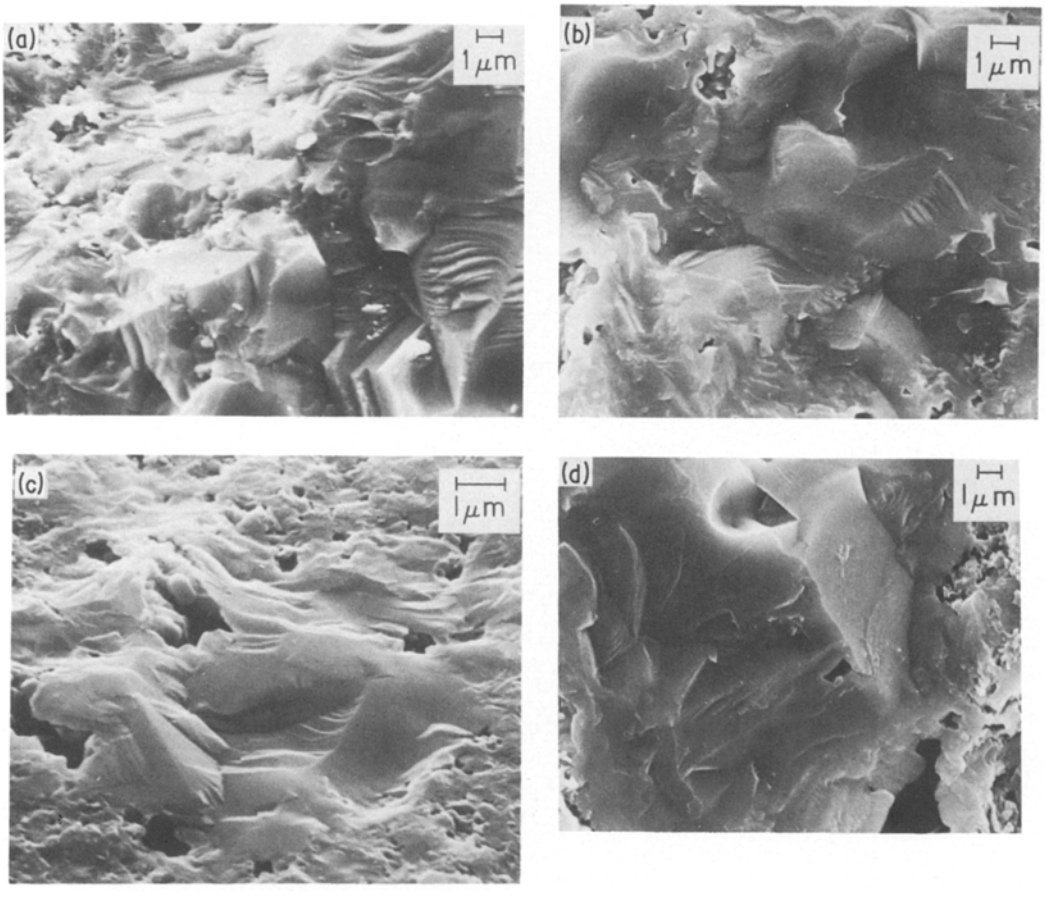

Figure 10 Example of typical fracture mode of RSSN. Note that there is substantial transgranular fracture in contrast to the predominantly intergranular fracture of hot pressed Si_3N_4. Materials are (a) Boeing ($P \sim 50\%$), (b) KBI, ($P \sim 20\%$), (c) Boeing ($P \sim 19\%$), and (d) NC 350 ($P \sim 24\%$).

($< 40\%$) can typically be expressed by the exponential relationship, $\gamma = \gamma_0 \exp^{-bp}$ where γ is the fracture energy at any volume fraction porosity P, γ_0 is the fracture energy at $P = 0$, and b is a constant which is the slope of a semi-log plot of γ against P. Based on other studies the typical b value for γ would be 4 ± 2, which is also the same as found for more extensive studies of both Young's modulus and flexure strength of ceramics [4] as well as Si_3N_4 [3] as a function of porosity (Figs. 6 and 7). Such values are also consistent with more probable theoretical values of 3 to 5 [4]. Lines with slopes $b = 3$, 4 or 5 drawn through the centroid of the data for bodies with $P < 0.4$ (i.e. excluding those in group B) extrapolates to $\gamma_0 \sim 20$ to $30\,J\,m^{-2}$ for pure dense Si_3N_4. Thus, note that extrapolation of K_{IC} and γ for RSSN are consistent with the γ of 20 to $30\,J\,m^{-2}$ for pure, dense fine grain Si_3N_4 based upon the extrapolations of fracture energy of HPSN to zero volume per cent additions.

4.1.3. CVD Si_3N_4

The fracture energy of CVD Si_3N_4 at first increases with web thickness, then levels off at 25 to $30\,J\,m^{-2}$ (Fig. 11) consistent with the extrapolations of HSPN and RSSN results to pure dense Si_3N_4. This γ-web thickness behaviour is attributed to cracks not encompassing a sufficient number of grains at smaller web thicknesses to reflect the true polycrystalline value. Thus, as the web thickness decreases so the crack encompasses fewer and fewer grains, it approaches the lower single crack crystal value of γ as shown in other ceramics [27]. Variations in microstructure, composition, and residual stresses (indicated by some cracking) are factors in the data scatter. However, the basic agreement between materials from three sources (and at least two lots from one source) strongly argue that the observed trend is that of Si_3N_4 and not an artifact of factors leading to the scatter.

The crystalline phase and its possible interaction

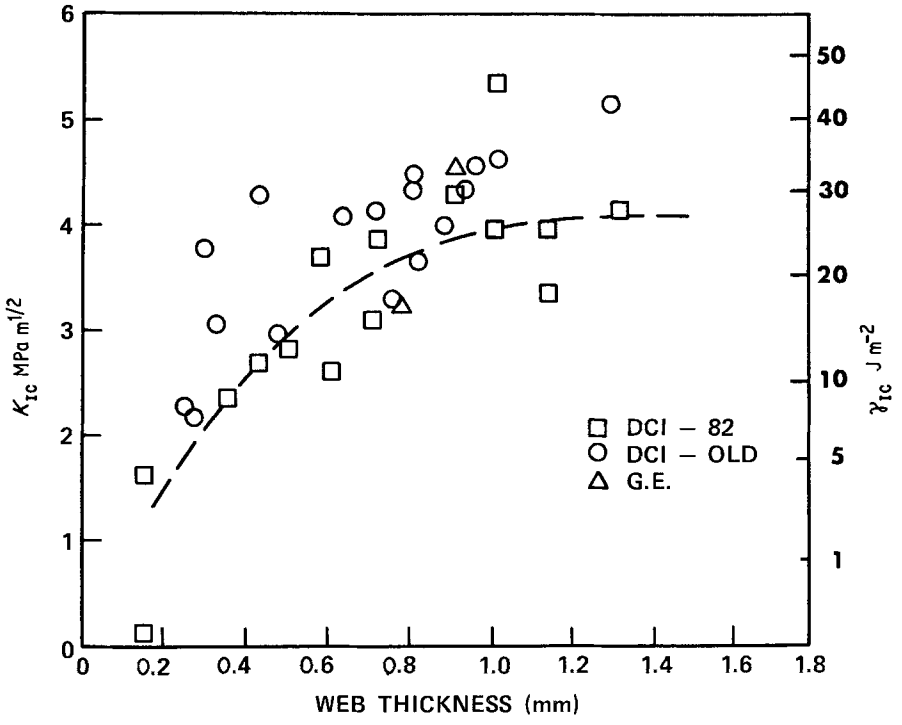

Figure 11 Fracture toughness against DCB web thickness in CVD, Si_3N_4. Data are shown for two sources of material. The line shown is the best visual fit to the most recent DCI material which was more consistent, e.g. there was less cracking in the as-deposited Si_3N_4.

with larger grain sizes must also be considered in comparing CVD and other Si_3N_4 bodies. CVD Si_3N_4 is predominantely α-Si_3N_4, whereas most hot pressed bodies are predominantely β-Si_3N_4. However, earlier [9], as well as more recent studies [12, 13, 15, 16] show no significant effect of varying α and β contents on the fracture energy of RSSN, questioning whether the α, β contents alone are a significant factor, even in larger grain bodies. (However, in HPSN development of elongated β grains has been associated with conversion from mainly α phase powder to dense β-Si_3N_4 and resultant higher γ values as noted earlier.)

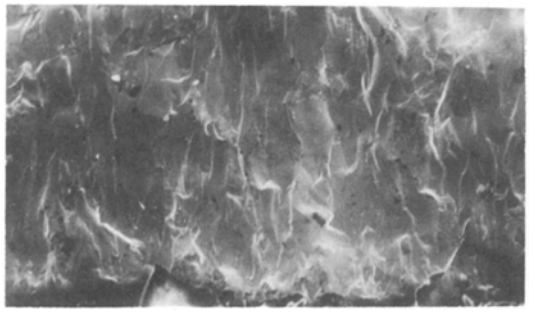

Figure 12 Fracture microstructure of GE CVD Si_3N_4. Photo taken from DCB fracture surface near the edge that was in contact with the graphite substrate from which the sample was removed for test.

Recent studies [5, 28] have shown that thermal expansion anisotropy can result in γ increasing, passing through a maximum and then decreasing as grain size increases. However, two factors show that this does not appear to be significant with CVD Si_3N_4. First the X-ray microradiographic studies of CVD Si_3N_4 show no evidence of microcracking or crack branching which is the cause of fracture energy changes with grain size observed in noncubic materials [4, 5]. This is consistent with the second factor; namely, that α-Si_3N_4 has extremely limited thermal expansion anisotropy, e.g. less than 3% difference in expansion between the *a* and *c* directions to 1000° C [29]. The extensive transgranular failure in the large grain CVD bodies (Fig. 9) is also consistent with the rather limited anisotropy of α-Si_3N_4. Significant thermal expansion anisotropy would be expected to result in substantial grain boundary stresses which would enhance intergranular failure at large grains, as observed in Al_2O_3 [30]. Thus, since neither the high α content of CVD Si_3N_4 nor its large grain size appear to have a significant effect on its fracture energy, the CVD data also support an intrinsic

fracture energy of 20 to 30 J m^{-2} for pure dense Si_3N_4.

While the intrinsic γ of Si_3N_4 is in the range 20 to 30 J m^{-2} a single γ value in this range may not be appropriate for all dense Si_3N_4. Factors such as grain size and shape as well as phase content, while not major factors, may be sources of second order effects within this range of 20 to 30 J m^{-2}. As noted earlier, grain elongation has been correlated with higher γ values in HPSN. However, this was clearly not the case for the CVD Si_3N_4. Thus grain elongation, by itself, does not necessarily lead to high γ values. However, grain boundary phases which enhance intergranular fracture around large grains should be important in raising fracture energies over those obtained with equiaxial grains with grain boundary phases.

4.2. Strength and Young's modulus behaviour

Strength and (Young's modulus of RSSN) results reinforce the previous γ results. Thus, earlier studies [20] found that strengths of HSPN with large γ values were not as high as would be expected for such γ values. This discrepancy was attributed to heterogeneities leading to weaker areas controlling strength [20]. However, more recent work has shown that such high γ values are associated with crack branching [7]. This in turn leads to the recognition that such branching may often require a scale of crack propagation greater than that for typical strength controlling flaws, and hence another reason why such higher γ values would not translate into higher strengths [26]. As yet the mechanism responsible for the γ-strength differences cannot be resolved, however two points should be noted. First, the crack branching distance argument is consistent with RSSN results discussed below. Second, crack branching in γ tests often results from microcracking [7, 26] and hence can be consistent with modelling of γ values based on microcracking as noted earlier.

The strength and Young's modulus of RSSN corroborate the basic porosity dependence of mechanical properties of Si_3N_4, as noted earlier, showing that some γ–P behaviour is anomalous. It is also clear that the crack branching associated with anomolously high γ values is on a scale larger than the typical flaws controlling strength of RSSN. Thus, as noted above for HPSN, the scale of this source of higher γ values is simply not compatible with normal strength controlling flaws. More generally, note that extrapolations of not only the RSSN strengths of this study, but also of other studies (Fig. 7), to $P = 0$, all give strengths that are consistent with an intrinsic γ (i.e. at $P = 0$) of 20 to 30 J m^{-2} for the typical range of flaw sizes (20 to 50 μm) found in Si_3N_4 [20, 31, 32] and most other technical ceramics [32]. Further, the more probable $P = 0$ extrapolated strengths of 350 to 420 MPa are in excellent agreement with strengths that Palm and Greskovich [23] measured on their single phase, dense HPSN bodies, as were their γ values (as noted earlier).

Finally, note that the lower CVD Si_3N_4 strengths (Table II) are consistent with the limited crack-size sampling of grains noted earlier in discussion of CVD γ values. The strength controlling flaw sizes expected, as well as seen [33] in these bodies, are smaller than the grains. Thus, based on other studies [27] of this same flaw-grain size phenomena, strengths of the CVD bodies should be controlled by γ transitioning to single crystal values for observed transgranular fracture and hence lower γ values as found. This is also consistent with the greater grain size dependence of strength in this and other studies [34] in this larger grain size range.

4.3. Correlation with SiC, and development implications

The implication of this work that oxide additives used to densify Si_3N_4 also contribute to its fracture toughness; i.e. making it a composite material, is reinforced by recent studies of SiC. Fracture energies of SiC hot pressed with oxide additives such as Al_2O_3, BeO, or MgO increase from 20 to 30 J m^{-2} for "pure" SiC to a maximum of $\geqslant$ 60 J m^{-2}, at significant e.g. (30 to 50%) additive contents [35, 36]. The large amounts of oxide additions needed to produce such increases in γ in SiC relative to those for similar increases in Si_3N_4 are generally consistent with the higher thermal expansion of SiC, and hence less mismatch with oxide grain boundary phases in SiC [19].

These results have two important implications for further development of Si_3N_4 and SiC. First, use of larger amounts of "densification aids" such as MgO should be beneficial to applications, e.g. in bearings, requiring good lower temperature, but not high temperature toughness and strength. Second, use of additives, e.g. non-oxides, that can be used in substantial quantity, yet be less detrimental to high temperature properties, should be

sought. Use of such additives to give grain boundary phases with substantial thermal expansion coefficient differences from Si_3N_4 or (SiC) should give rise to high K_{IC} as achieved with oxide additions, but with substantially reduced compromise of mechanical properties at higher temperature.

5. Summary and conclusions

Studies of the fracture energy and strength of hot pressed, reaction sintered, and CVD Si_3N_4 all show that the intrinsic fracture energy of dense, pure, Si_3N_4 is 20 to 30 J m^{-2}. A single value in this 20 to 30 J m^{-2} may not be appropriate for dense bodies due to possible effects of factors such as phase content, grain size, and shape. Values higher than this range for dense bodies, and than those expected from normal porosity dependence in RSSN, are related to crack branching. Such branching is often related to, and probably is a more advanced stage of, microcracking. Much of the scale of such crack branching is too large to be operative with normal strength controlling flaws, and hence strengths do not scale with γ for higher γ values of hot pressed or reaction sintered bodies (for a given porosity). The results show that bodies hot pressed (or sintered) with additives can often be viewed as composites in which the additives not only aid densification, but can increase fracture energies, due to differences in properties between the additive and Si_3N_4.

Acknowledgements

This work was supported by the Naval Air Systems Command, Irv Machlin Contracting Officer. Messrs F. Simpson, and J. Verzemnieks of Boeing Co, kindly provided RSSN samples for this study, as well as their strength data for comparison with this study, while their colleague T. Basu provided K_{IC} (NB) data. The authors also wish to thank R. Baumgartner (then at the Norton Co), K. Komeya (Toshiba), and R. Palicka (Ceradyne) for samples of various hot pressed Si_3N_4 bodies.

References

1. F. F. LANGE, *J. Amer. Ceram. Soc.* **56** (1973) 518.
2. G. HIMSOLT and H. KNOCH, *ibid.* **62** (1979) 29.
3. R. W. RICE and S. W. FREIMAN, in "Ceramic Microstructures '76", edited by R. M. Fulrath and J. A. Pask (Westview Press, 1976) p. 800.
4. R. W. RICE, "Treatise on Materials Science and Technology", Vol. 11, edited by R. K. MaCrone (Academic Press, New York, 1977) 199.
5. R. W. RICE, S. W. FREIMAN and P. F. BECHER, *J. Amer. Ceram. Soc.* **64** (1981) 345.
6. R. W. RICE and W. J. MCDONOUGH, *ibid.* **58** (1975) 264.
7. S. W. FREIMAN, D. R. MULVILLE and P. W. MAST, *J. Mater. Sci.* 8 (1973) 1527.
8. C. CM. WU, S. W. FREIMAN, R. W. RICE and J. J. MECHOLSKY, *ibid.* **13** (1978) 2659.
9. C. CM. WU, R. W. RICE and P. F. BECHER, in "Fracture Mechanics Methods for Ceramics, Rock and Concrete", ASTM STP 745, edited by S. W. Freiman and E. R. Fuller Jr, (American Society for Testing Materials, Philadelphia, 1981) p. 127.
10. A. G. EVANS and R. W. DAVIDGE, *J. Mater. Sci.* **5** (1970) 314.
11. J. A. COPPOLA, R. C. BRADT, D. W. RICHERSON and R. A. ALLIEGRO, *Amer. Ceram. Soc. Bull.* **51** (1972) 847.
12. B. J. DALGLEISH and P. L. PRATT, *Proc. Brit. Ceram. Soc. Mechanical Properties of Ceram. (2)* Δ 25, edited by R. W. Davidge, May (1975) p. 295.
13. S. C. DANFORTH, H. M. JENNINGS and M. H. RICHMAN, *Acta Metall.* **27** (1979) 123.
14. D. C. LARSEN, "Illinois Institute Technical Research Materials Semiannual Interim Technical Report No. 7" prepared for Air Force Materials Laboratory, Contract F33615-75-C-5196, March 1979.
15. J. HEINRICH, "Der Einflub von Herstellungsbedingungen auf das Gefuge und die mechanischen Eigenschaften con reaktionsgesintertem Siliciumnirid," Deutsche Forschungs-und Cersuchsanstalt Luft-und Raumfahrt Report DFVLR-FB79-32, September 1979.
16. J. HEINRICH and D. MUNZ, *Bull. Amer. Ceram. Soc.* **59** (1980) 1221.
17. R. W. RICE, *J. Mater. Sci.* **12** (1977) 627.
18. J. W. EDDINGTON, D. J. ROWCLIFFE and J. L. HENSHALL, *Powder Metallurgy Int.* 7 (1975) 82.
19. R. W. RICE, in press.
20. S. W. FREIMAN, A. WILLIAMS, J. J. MECHOLSKY and R. W. RICE, in "Ceramic Microstructures '76", edited by R. Fulrath and J. Pask (Westview Press, 1976) 824.
21. G. BANSAL, *ibid.*, p. 860.
22. P. F. BECHER, *J. Amer. Ceram. Soc.* **59** (1976) 59.
23. J. A. PALM and C. D. GRESKOVICH, *Amer. Ceram. Soc. Bull.* **59** (4) (1980) 447.
24. M. SHIMADA and M. KOIZUMI, *J. Amer. Cer. Soc.* **65** (4) (1982) 48.
25. S. C. DANFORTH, H. M. JENNINGS and M. H. RICHMAND, *J. Mater. Sci.* **13** (1978) 1590.
26. R. W. RICE, *ibid.* **13** (1978) 2659.
27. R. W. RICE, S. W. FREIMAN and J. J. MECHOLSKY JR, *J. Amer. Ceram. Soc.* **63** (3–4) (1980) 129.
28. R. W. RICE and S. W. FREIMAN, *ibid.* **64(6)** (1981) 350.
29. C. M. B. HENDERSON and D. TAYLOR, *Trans. J. Brit. Ceram. Soc.* 74 (1975) 49.
30. R. W. RICE, "Surfaces and Interfaces of Glass and Ceramics", edited by V. D. Frechette, W. C. LaCourse and V. L. Burdick (Plenum Press, New York, 1974) 439.
31. R. W. RICE, S. W. FREIMAN, J. J. MECHOLSKY

Jr, R. RUH and Y. HARADA, "Ceramics for High Performance Applications II", edited by J. J. Burke, E. N. Lenoe, and R. N. Katz, (Brook Hill Publishing Co. Chestnut Hill, MA, 1978) p. 699.
32. R. W. RICE, S. W. FREIMAN, J. J. MECHOLSKY Jr and R. RUH, in the Proceedings of the 1977 DARPA/NAVSEA Ceramic Gas Turbine Engine Demonstation Program Review, edited by J. W. Fairbanks and R. W. Rice (Battelle, Columbus MCIC-78-36, March 1978) p. 665.
33. R. W. RICE and J. J. MECHOLSKY Jr, "The Science of Ceramic Machining and Surface Finishing II" edited by B. J. Hockey and R. W. Rice, (National Bureau of Standards Special Publication 562, October 1979) p. 351.
34. "Processing Research on Chemically Vapour Deposited Silicon Nitride-Phase 2" General Electric Co Re-Entry Systems Division Technical Report, February 1978–October 1979, Office of Naval Research, Contract No N00014-78-C-0107, December 1979.
35. R. W. RICE, P. F. BECHER, S. W. FREIMAN and W. J. MCDONOUGH, *Ceram. Eng. Sci. Proc.* 1 (1980) 424.
36. D. LEWIS and P. F. BECHER, *ibid.* 1 (1980) 634.

Received 31 October 1983
and accepted 23 October 1984